

# Fourier Transform Photocurrent Spectroscopy on hydrogenated amorphous silicon

M. Verbaan, G. van Elzakker and M. Zeman  
Delft University of Technology, Dimes  
P.O. Box 5053, 2600 GB Delft, the Netherlands  
Phone: +31 (0)15 2781651 Fax: +31 (0)15 2622163  
E-mail: [m.verbaan@gmail.com](mailto:m.verbaan@gmail.com)

**Abstract—** In this paper the Fourier transform photocurrent spectroscopy (FTPS) measurements of amorphous silicon films and solar cells are presented. Experimental conditions for deposition of amorphous silicon films and solar cells and procedures on how to obtain the defect concentration via the absorption coefficient are described. The results from FTPS are discussed and compared with Dual Beam Photoconductivity (DBP) and current and voltage (IV) measurements.

**Keywords—** a-Si:H; solar cells; Fourier Transform Photocurrent Spectroscopy; absorption coefficient;

## I. INTRODUCTION

Hydrogenated amorphous silicon (a-Si:H) solar cells are receiving increasingly more interest from the solar cell community because of their potential cost-effective production and a-Si:H modules approaching efficiencies of 10%.

Unlike crystalline silicon, a-Si:H has a short range order in its atomic structure resulting in a continuous random network in which some silicon atoms have only three covalent bonds. A silicon atom that has one valence electron unpaired represents a (coordination) defect in a-Si:H, which is described as a dangling bond. Dangling bonds can be classified in three charged states (+, 0, -) depending on the number of electrons attached to the defect. Defects are inherent to the a-Si:H structure and they act like trapping or recombination sites decreasing the carrier lifetime. Therefore, defects in an a-Si:H absorber layer strongly influence the performance of an a-Si:H solar cell.

The concentration of defects in pure a-Si can become quite significant, usually in the range of  $10^{21}$  defects/cm<sup>3</sup>, making this material inappropriate for electronic devices. By hydrogenating the material the defect concentration can be decreased by 5 to 6 orders of magnitude, making it possible to use a-Si:H films in electronic devices. Apart from the concentration of defects in a-Si:H it is also important to know how the energy states, introduced by the defects, are distributed in the band gap. [1],[2].

In 1977 D.L. Staebler and C.R. Wronski published a paper on what they called a reversible photoelectronic effect in amorphous silicon. This effect, now called the Staebler Wronski effect (SWE) [3],[4], consists of an increase in defect concentration, due to exposure to light which can be reversed by annealing above 150 °C. The creation of extra defects in a-Si:H due to illumination causes a drop in the solar cell performance. However, the defect concentration saturates after some time, which means that a solar cell will eventually achieve a so-called stabilized efficiency.

There are several methods of determining the defect concentration and/or the distribution of defect states in a-Si:H. These methods can be divided into the following groups. The methods of the first group use the properties of a space-charge region that is formed at the interfaces of a-Si:H with other materials. By filling the defects in the space-charge region and then discharging them as is done with *Charge-Deep-Level Spectroscopy* (Q-DLTS) one can determine the distribution of the defect states [5],[6]. A second group is based on correlating the optical absorption in a-Si:H films or devices with the density of states distribution. Especially the sub-band gap absorption is of major interest since it reflects transitions involving the localized states within the band

gap. However, the sub-band gap absorption is weak and therefore indirect methods, which are based on measurement of some secondary effect, are used to determine the absorption coefficient. In *Photothermal Deflection Spectroscopy* (PDS) [7], the deflection of a probe laser beam reflects a change in the refractive index of a medium which is in contact with the a-Si:H film. The change of the refractive index depends on the amount of heat generated by the absorption of monochromatic light in the a-Si:H film and dissipated from the film into the medium. Other techniques, such as the *Constant Photocurrent Method* (CPM) [8], *Dual Beam Photoconductivity* (DBP) [9], and recently introduced *Fourier Transform Photocurrent Spectroscopy* (FTPS) [10] are based on measurement of the spectral dependence of the photoconductivity. FTPS uses the interferometer and light source of a *Fourier Transform Infrared Spectroscopy* (FTIR) spectrometer and an a-Si:H sample as the detector. CPM, DBP and PDS use a monochromator and measure the photocurrent for one wavelength at a time. The use of an interferometer is the main reason why FTPS is faster and more sensitive than CPM or DBP. An interferometer allows the user to measure all wavelengths at once instead of one at a time like the monochromator does. Results of FTPS, used on microcrystalline silicon solar cells and layers, have been published and demonstrate that FTPS combines high sensitivity with fast measuring times [11],[12].

In this paper we report on the FTPS measurements on amorphous silicon layers and solar cells. Since the FTPS is a fast measuring technique it is possible to measure a set of solar cells deposited on one substrate and carry out a statistical analysis. We have chosen to use FTPS to study the degradation of a-Si:H solar cells and correlate the changes observed in the sub-band gap absorption with the external parameters of the degraded solar cells.

We have analyzed the degradation of a-Si:H using three series. The first series consisted of a-Si:H layers with different layer thicknesses (300, 600, 900 nm). The second series represents a-Si:H solar cells in which the thickness of the intrinsic a-Si:H layer was varied in the same way as the thickness of the layers in the first series. The third series includes a-Si:H solar cells in which the intrinsic absorber layer was deposited at two different hydrogen dilutions of the silane source at deposition ( $R = 0$  and  $R = 20$ ).

The dilution ratio,  $R$ , is defined as:

$$R = \frac{[H_2]}{[SiH_4]} \quad (1)$$

The two different absorber layers were applied in the solar cell in two different thicknesses 300 nm and 1000 nm, respectively. The last series was prepared because results in literature [5] show that diluting silane with hydrogen could result in a-Si:H material which in solar cells is less sensitive to light soaking degradation.

## II. THEORY

### A. Absorption coefficient

The absorption coefficient curve  $\alpha(E)$  of a-Si:H can be divided into three separate regions I, II and III (see figure 1) [13],[14]. Region III ( $E > 1.6$  eV) is the part of the coefficient where absorption is dominated by transitions between the extended states of the valence and conduction bands.

An exponential dependence of the absorption coefficient on photon energy is observed in region II (1.1 eV – 1.6 eV). In this region the transitions between the valence and conduction band tail states dominate. The absorption in this region extends over 4 orders of magnitude and can be described by:

$$\alpha(E) = \alpha_0 \exp\left(\frac{E}{E_0}\right) \quad (2)$$

where  $\alpha_0$  is a scaling constant and  $E_0$  is the Urbach energy [15]. The Urbach energy  $E_0$ , which for device quality a-Si:H is less than 0.05 eV [16][17], determines the slope of the absorption coefficient energy dependence and is a figure of merit for the amount of disorder in a-Si:H material [18].

Region I ( $E < 1.1$  eV) reflects the so called sub-band gap absorption where the transitions between the defect states and the conduction band take place, so a high absorption in this region could indicate a high defect density [19].

In order to obtain information about the defect concentration in the material from the absorption coefficient three methods are used [20]: (i) deconvolution of the sub-band gap absorption spectrum, (ii) the value of absorption at 1.2 eV, and (iii) integrated sub-band gap absorption.

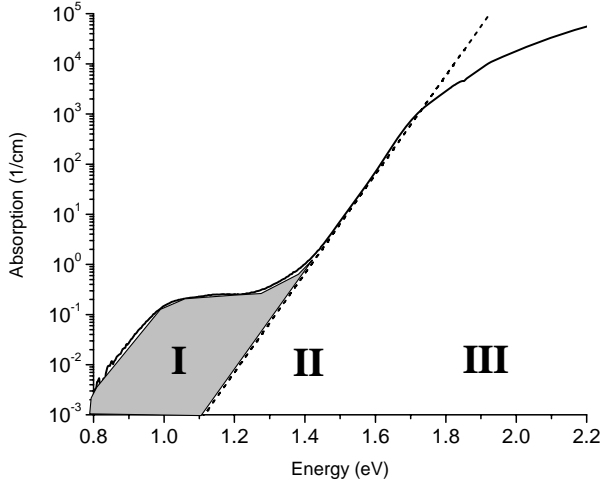


**Figure 1 Absorption curve of amorphous silicon including Urbach line ( $E_0 = 0.045$  eV)**

With the first method one tries to find the defect distribution by changing parameters in a model until it fits the measured absorption:

$$\alpha(E) = \frac{\text{constant}}{h\nu} \int N(\varepsilon)g(\varepsilon + E)d\varepsilon \quad (3)$$

where  $N(\varepsilon)$  is the density of all initial states (valence band extended and tail states and defect states) and  $g(\varepsilon + E)$  is the density of the final extended states in the conduction band. A few assumptions are made such as a parabolic energy dependence of the extended conduction band states, an exponential energy dependence of valence band tail states and a Gaussian distribution of defect states. These assumptions give the following absorption coefficient due to defect state transitions [21]:

$$\alpha_d(E) = N_c \frac{A}{\sqrt{2\pi W^2}} \frac{\text{constant}}{E} \int \frac{\exp(-[\varepsilon - E - E_i]^2)}{2W^2} d\varepsilon \quad (4)$$

where  $N_c$  is the effective density of states at the conduction band,  $E_i$  is the energy position of the peak of Gaussian defect distribution relative to the conduction band,  $W$  is the half width of the Gaussian distribution and  $A$  is the area of the Gaussian distribution. By varying  $A$  when fitting the equation (4) the defect density can be found.

The second method evaluates the absorption coefficient at 1.2 eV. This value is expected to be a measure for the concentration of neutral dangling bond defects  $D^0$  in the a-Si:H material. Often this value is used as a measure of the total concentration of defects. The

value of 1.2 eV is chosen because at this energy the photon induces transitions from defect states into the conduction band states, but it will not induce transitions from the valence band tail states into the conduction band states. This method is only useful when the absorption coefficient curve does not exhibit interference fringes.

The third method uses the sub-band gap absorption region, indicated in figure 1, to obtain the concentration of defects by integrating the region as a function of photon energy. The integrated sub-band gap absorption has a few drawbacks such as that the integral depends strongly on how the Urbach energy is determined (figure 1). We use the last described method in this paper to determine the defect concentration in the samples. This method is chosen, because the first method consumes too much time and the second one is too sensitive for the interference fringes in the absorption coefficient.

### B. FTFS

The heart of the FTFS setup is the FTIR spectrometer, which is a two beam interferometer similar to the interferometer designed in 1891 by Michelson (figure 2). The interferometer creates interference by introducing a path difference between two beams of monochromatic light. The two beams are produced by the beamsplitter which partially reflects and partially transmits the incident light, thus creating two light beams. A path difference (retardation) is created by moving one of the mirrors ( $m$ ) while the second mirror is fixed ( $f$ ). The retardation between both mirrors is  $2(OM-OF)$  at the detector (see figure 2). When the retardation is 0, the two beams will be in phase and interfere constructively. If the mirror  $m$  is displaced  $\lambda/4$  the retardation will be  $\lambda/2$  and the beams will interfere destructively. This means that when the retardation is an integer multiple of  $\lambda$  a maximum signal is detected and a minimum signal is detected for an odd integer multiple of  $\lambda/2$ .

When the mirror  $m$  moves at a constant speed the detected interferogram will be:

$$I(\delta) = \int_0^{\infty} B(\bar{\nu}) \cos(2\pi\delta / \lambda) d\bar{\nu}, \quad (5)$$

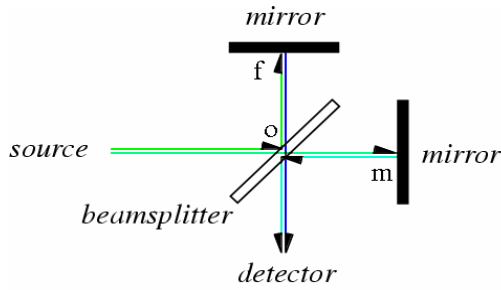


**Figure 2** Michelson interferometer where the mirror  $m$  moves at a constant speed while the mirror  $f$  is fixed at one position, creating a path difference.

where  $\delta$  is the retardation and  $B(\nu)$  is the combined spectral characteristic of the light source, beamsplitter and mirrors. Because the mirror  $m$  moves at a constant speed it is possible to see how the detected intensity changes as a function of time:

$$\delta = 2Vt, \quad (6)$$

where  $V$  is the speed at which the mirror  $m$  is moving. Combining (5) and (6) gives us:

$$I(t) = \int_0^{\infty} B(f_{\nu}^-) \cos(2\pi \bar{\nu} \cdot 2Vt) df_{\nu}^- \quad (7)$$

$I(t)$  is the cosine Fourier transform of  $B(f_{\nu}^-)$ , hence the name *Fourier Transform Photocurrent Spectroscopy*.

Just like other methods based on measurement of the photocurrent, FTPS does not give an absolute value for the absorption coefficient. The results have to be calibrated by the absorption coefficient curve obtained from a reflectance transmittance (RT) measurement. This calibration is carried out in the region ( $\sim 1.8$  eV) where FTPS and RT overlap. The RT measurement is performed by illuminating a sample with monochromatic light and measuring the fraction of reflected and transmitted light using Si/Ge photodiodes. The results of the FTPS measurement on a solar cell with a 900 nm thick intrinsic layer were first compared to those of DBP (see figure 3). Figure 3 shows that the FTPS and DBP measurements resulted in similar absorption coefficients. The DBP measurement has more pronounced interference fringes but the overall trend of the determined absorption coefficient is the same comparing to the FTPS measurement. While DBP resolution reaches its limit at 0.8 eV, FTPS is able to measure reliably as low as 0.6 eV.

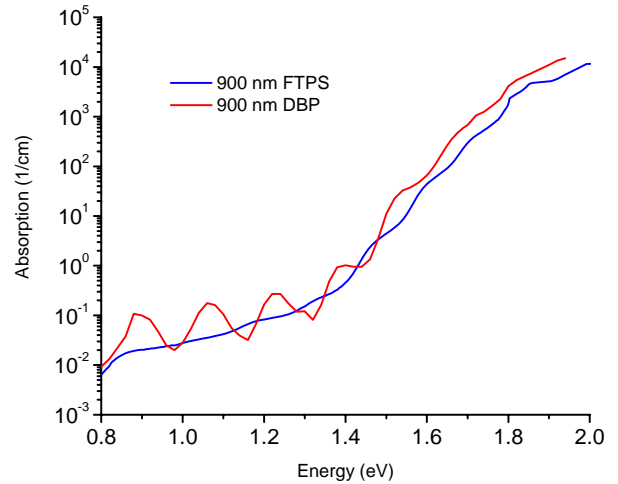


**Figure 3** Comparison of FTPS measurement and DBP measurement on 900 nm thick amorphous silicon solar cell.

A reasonable matching between the DBP and FTPS measurements proved that FTPS can be used for the measurements of a-Si:H samples discussed in this paper.

### III. EXPERIMENTAL

#### A. FTPS

The Thermo Nicolet 5700 FTIR spectrometer is used for the FTPS measurement. The interference beam is created using a  $\text{CaF}_2$  beamsplitter from the 20 W halogen white light source. The beam is focused onto a sample from which the resulting photocurrent is amplified by a Stanford SR 570 current preamplifier. For a-Si:H layers the voltage over the contacts is supplied by a Keithley voltage supply. After amplification a Fourier transform is performed to obtain the absorption coefficient.

In order to improve the dynamic range of the FTPS measurement, the measurement is carried out in different spectral regions. These regions are created using long pass optical filters. Connecting the measurements of the different spectral regions afterwards results in an absorption coefficient with a high dynamic range.

In order to correct the FTPS photocurrent signal for the characteristics of the used components (beamsplitter, mirrors and lamp) a reference measurement is performed using a DTGS detector instead of a a-Si:H sample. By normalizing the sample measurement by the reference measurement and scaling with the absorption curve obtained from a RT measurement the absorption of the sample is obtained.

After the FTPS measurements are scaled the absorption coefficient is corrected for the frequency dependence of the DTGS detector and amorphous silicon sample. All detectors have their own frequency dependence as a consequence of their physical properties. Since the intensity of the FTPS photocurrent signal varies with modulation frequency and every frequency varies with wavenumber each point in the collected data will have a different modulation frequency. Because FTPS uses different detectors for the measurement of the sample and for the reference measurement, the response of the DTGS detector and sample have to be corrected for their own frequency responses [10].

The interference fringes are removed by using the absorbance transmittance ratio method as proposed by Ritter and Weiser [22].

### B. DBP

For the DBP measurement a monochromatic light beam is produced using a 100 W halogen lamp combined with a Spex 1680B double grating monochromator. The monochromatic light is chopped at 13 Hz and split into two equal beams. One beam illuminates the sample while the other beam is measured by a Si/Ge photodiode to determine the incident photon flux. Bias light was applied with a wavelength larger than 800 nm.

### C. RT

In the RT measurements monochromatic light that is produced by an Eta Optic spectrometer, incidents perpendicular on the sample and the reflected and transmitted fraction of light is measured by two Si/Ge photodiodes.

### D. IV

IV measurements on the solar cells were performed under AM1.5 spectrum and a power density of  $100 \text{ mW/cm}^2$  delivered by an Oriel Corporation solar simulator. A Hewlett Packard 4145B semiconductor parameter analyzer is used to carry out the IV measurement.

### E. Deposition

The first series consists of undoped a-Si:H layers with a thickness of approximately 300, 600 and 900 nm deposited on Corning 1737 glass substrates by *Radio Frequency Plasma Enhanced Chemical Vapor Deposition* (rf-PECVD). The deposition conditions were; a substrate temperature of 467 K, a radio frequency of 13.56 MHz, a deposition pressure of 0.7 mbar, a silane flow of 40 sccm, and a power density

of  $\sim 16 \text{ mW/cm}^2$ . The resulting deposition rate was of  $2.2 \text{ \AA/s}$ . In order to carry out the photocurrent measurements, 500 nm thick aluminum contacts were deposited on the surface of a-Si:H layers using electron beam evaporation. The aluminum contacts are 4 mm wide and are separated by 0.5 mm from each other. The samples were annealed at 323 K for 45 minutes to reduce the contact resistance of the contacts

Single junction a-Si:H solar cells were deposited on Asahi U-type substrates using rf-PECVD at a temperature of 467 K. The solar cells have the following structure: a 10 nm p-type doped a-SiC:H layer, an intrinsic absorber layer and a 20 nm n-type a-Si:H layer. The back contact consists of a 100 nm silver layer with a 200 nm aluminum layer on top of silver layer. A series of solar cells was fabricated in which the thickness of the intrinsic layer was varied (300, 600 and 1000 nm). The deposition conditions used for the intrinsic layers in solar cells were equal to those used for the individual layers deposited on the glass substrate.

An additional series of solar cells was made with intrinsic layers deposited from silane diluted with hydrogen. The thickness of the intrinsic layer was 300 nm and 1000 nm, respectively. For these absorber layers a hydrogen to silane dilution ratio of  $R = 20$  was achieved by reducing the  $\text{SiH}_4$  flow to 5 sccm and introducing an additional  $\text{H}_2$  flow of 100 sccm. The deposition pressure and rf power density were changed to 2.0 mbar, and  $\sim 76 \text{ mW/cm}^2$ , respectively.

### F. Light soaking

For the light soaking experiments a 670 nm semiconductor laser was used with a power density of  $160 \text{ mW/cm}^2$ . All samples were light soaked for 30 minutes.

## IV. RESULTS

In [figure 4](#) the results of the FTPS measurements on the 300, 600 and 900 nm thick a-Si:H layers in as-deposited and light-soaked states are presented. We observe that the degradation of the three layers is not equal. When evaluating ([table 1](#)) the defect concentrations of the a-Si:H silicon layers we conclude that the thicker layers have a lower initial defect concentration.

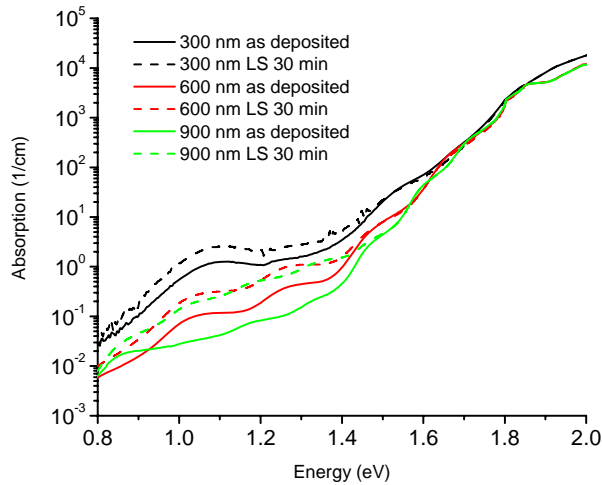


Figure 4 300, 600 and 900 nm thick amorphous silicon layers before and after light soaking.

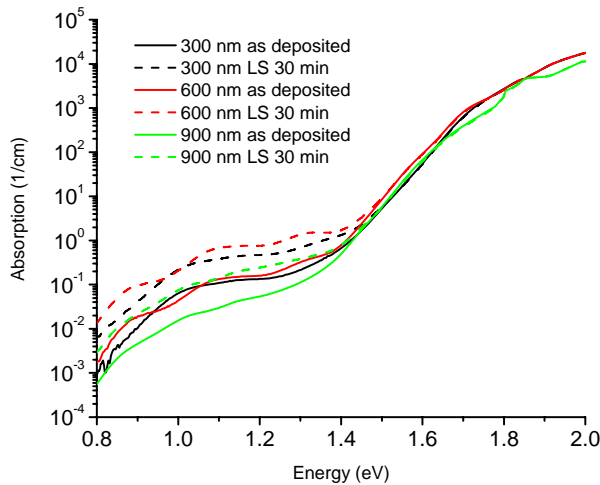


Figure 5 300, 600 and 900 nm thick amorphous silicon solar cells before and after light soaking.

The difference in the initial defect concentrations is probably caused by an inhomogeneous growth of the material. The initial growth can be characterized by a material with a high defect concentration. During the growth the material improves and the defect concentration decreases, resulting in a lower average defect concentration for thicker layers.

The defect concentration due to light soaking increases with a factor of 1.8, 3.5 and 17.6 for the 300 nm, 600 nm and 900 nm thick layers, respectively. Even though the relative increase of defects for the thicker layers is quite significant, a final defect concentration of  $5 \cdot 10^{15} \text{ cm}^{-3}$  is still an excellent value for device quality ( $< 10^{16} \text{ cm}^{-3}$ ) a-Si:H film.

The absorption coefficients determined by FTPS on the 300, 600 and 900 nm thick amorphous silicon solar cells are shown in figure 5 and the results presented in table 2. The results in table 2 demonstrate that the defect concentration increases with a factor of 4, 6 and 10 for the 300, 600 and 900 nm thick cells, respectively. The increase in the defect concentration as a function of the thickness of the intrinsic a-Si:H layer in solar cells follows the trend that is observed for the individual layers.

The defect concentrations determined from the measurements on solar cells are closer to each other for all three thicknesses of the absorber layers than those of the individual a-Si:H intrinsic layers. We expect that in the solar cell, the defect concentration in the a-Si:H intrinsic layer is not uniform but depends on the distance between the position of the Fermi level and the valence band edge. In the regions of the intrinsic layer close to the interfaces between the intrinsic layer and the doped layers the position of the Fermi level is close to the band gap edges. According to the defect pool model [1] in these regions the defect concentration is higher than in the region where the Fermi level is around midgap. We expect that the defect density in these interface regions are the same in all three solar cells and determines the average defect density.

Light soaking results in the increase of defect concentrations, and at the same time a decrease in the efficiency of solar cells. The creation of extra defects in the absorber layer results in the additional states in the band gap. These extra states act as additional recombination centers and cause a decrease in the current density and the fill factor of solar cells (see table 2).

The reason why the decrease in efficiency is smaller for solar cells with thinner absorber layers can be explained by the strength of the internal electric field across the intrinsic layer in the solar cell. The electric field facilitates the separation of the photo-generated carriers and sweeps them to the contacts. The strength of the electric field, which is built up by the p-type and n-type layers, depends on the thickness of the intrinsic layer. For thinner cells the electric field across the intrinsic layer is stronger and the cell is less influenced by the creation of extra defects due to the illumination.

FTPS and IV measurements were also carried out on a-Si:H solar cells in which the thickness (300 and 1000 nm) and dilution ( $R = 0$  and  $R = 20$ ) of the absorber layers was varied. The results of these measurements are shown in figures 6, 7 and table 3.

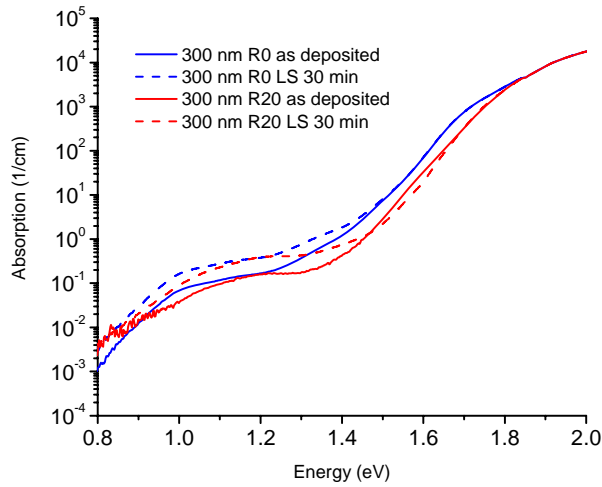


**Figure 6 300 nm thick solar cells with dilution R=0 and 20 before and after light soaking.**

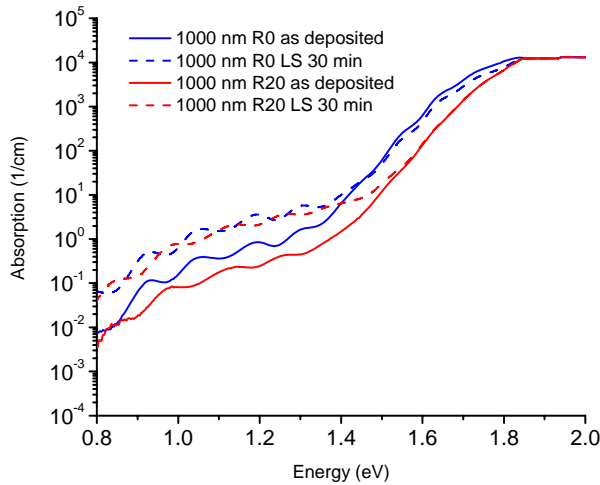


**Figure 7 1000 nm thick solar cell with dilution R=0 and 20 before and after light soaking.**

Observing [figure 6](#) and [table 3](#) we can notice that the initial defect concentrations and the open circuit voltage ( $V_{oc}$ ) of the 300 nm diluted and undiluted solar cells are similar, while the short circuit current ( $J_{sc}$ ) and the fill factor are different. The lower fill factor and  $J_{sc}$  in case of a diluted cell results in a lower initial efficiency of the diluted solar cell. After light soaking, the stabilized efficiency is still smaller for the diluted solar cell, however the relative change of all external solar cell parameters is smaller than those of the undiluted solar cell.

The absorption coefficient determined from the FTPS measurements on the 1000 nm thick solar cells are shown in [figure 7](#) and the external parameters determined from the IV measurement are presented in

[table 3](#). The defect concentration, fill factor, short circuit current and initial efficiency of the diluted solar cell are smaller than those of the undiluted cell. After light soaking the relative change of these parameters is lower in the case of a the diluted solar cell, as is also observed for the 300 nm solar cell. The only exception to this is the increase of the defect concentration. The increase of defects in the 1000 nm diluted cell is higher than that of the undiluted cell, however the relative change in efficiency is still lower. The lower relative changes in performance for the diluted solar cells confirm that solar cells with diluted intrinsic absorber layers are less sensitive to light soaking.

A concluding remark can be made about the discrepancy between the absorption coefficients ([figure 6](#) and [7](#)) of the diluted and undiluted cells at higher energies. This difference at higher energies can be explained by an increase of the optical band gap [23] due to the dilution with hydrogen. The Tauc band gap for the diluted absorber layer is 2.0 eV while a bandgap of 1.8 eV is determined for the undiluted a-Si:H layer.

**Table 1. Results of FTPS measurements on amorphous silicon layers before and after light soaking (bold).**

|  | 300 nm              | 600 nm              | 900 nm               |
|--|---------------------|---------------------|----------------------|
| Urbach energy (meV)                      | 50                  | 50                  | 50                   |
| Def. conc. ( $10^{16} \text{ cm}^{-3}$ ) | 1.06<br><b>1.90</b> | 0.13<br><b>0.46</b> | 0.025<br><b>0.44</b> |

**Table 2. Results of FTPS and IV measurements on amorphous silicon solar cells before and after light soaking (bold).**

|  | 300 nm                | 600 nm                | 900 nm                |
|--|-----------------------|-----------------------|-----------------------|
| Def. conc. ( $10^{16} \text{ cm}^{-3}$ ) | 0.095<br><b>0.39</b>  | 0.114<br><b>0.68</b>  | 0.017<br><b>0.17</b>  |
| Increase def. conc.                      | 4.1                   | 5.9                   | 10                    |
| Fill Factor                              | 0.70<br><b>0.58</b>   | 0.68<br><b>0.49</b>   | 0.63<br><b>0.42</b>   |
| $J_{sc}$ ( $\text{mA}/\text{cm}^2$ )     | -14.3<br><b>-13.5</b> | -15.5<br><b>-14.0</b> | -16.4<br><b>-13.3</b> |
| $V_{oc}$ (V)                             | 0.86<br><b>0.81</b>   | 0.85<br><b>0.80</b>   | 0.84<br><b>0.80</b>   |
| Eff (%)                                  | 8.74<br><b>6.38</b>   | 8.94<br><b>5.45</b>   | 8.80<br><b>4.60</b>   |
| Decrease eff.                            | 27 %                  | 39 %                  | 47 %                  |

**Table 3. Results of FTPS and IV measurements on diluted and undiluted amorphous silicon solar cells before and after light soaking (bold).**

|  | 300 nm<br>R0          | 300 nm<br>R20         | 1000 nm<br>R0         | 1000 nm<br>R20      |
|--|-----------------------|-----------------------|-----------------------|---------------------|
| <b>Def. conc.</b><br>( $10^{16} \text{ cm}^{-3}$ ) | 0.095<br><b>0.39</b>  | 0.095<br><b>0.23</b>  | 0.36<br><b>2.15</b>   | 0.15<br><b>2.10</b> |
| <b>Increase def. conc.</b>                         | 4.1                   | 2.4                   | 5.9                   | 14                  |
| <b>Fill Factor</b>                                 | 0.70<br><b>0.58</b>   | 0.62<br><b>0.54</b>   | 0.63<br><b>0.47</b>   | 0.51<br><b>0.45</b> |
| <b>Jsc (mA/cm<sup>2</sup>)</b>                     | -14.3<br><b>-13.5</b> | -12.5<br><b>-11.9</b> | -18.1<br><b>-16.3</b> | -15<br><b>-11.9</b> |
| <b>Voc (V)</b>                                     | 0.86<br><b>0.81</b>   | 0.84<br><b>0.82</b>   | 0.86<br><b>0.85</b>   | 0.87<br><b>0.87</b> |
| <b>Eff (%)</b>                                     | 8.74<br><b>6.38</b>   | 6.39<br><b>5.84</b>   | 9.81<br><b>6.68</b>   | 6.58<br><b>4.89</b> |
| <b>Decrease eff.</b>                               | 27 %                  | 9 %                   | 32 %                  | 26 %                |

## V. SUMMARY

Series of amorphous silicon solar cells and layers varying in thickness (300, 600 and 900 nm) and hydrogen dilution (R=0 and R =20) have been studied using FTPS.

The degradation of amorphous silicon layers (300, 600 and 900 nm) showed that the degradation is dependent on the thickness of the material.

The results of the amorphous silicon solar cells (300, 600 and 900 nm) show that the absorbing layer is not the same as the amorphous silicon layer, since defect concentrations do not correspond. This was explained by the Fermi level in the absorbing layer which influences the defect concentration.

FTPS can be used to compare individual solar cells and it was clear that the defect concentration for all solar cells was similar. But after looking at the IV measurements it was found that thinner solar cells react less to light soaking than thicker cells. This is due to the better collection of electrons in thin cells as a result of stronger electric fields.

Finally a series of amorphous silicon solar cells was measured varying in thickness (300 and 1000 nm) and dilution (R=0 and R=20). It was observed that the efficiency of diluted cells was lower than that of undiluted cells. However it was confirmed that for the diluted solar cells the sensitivity to light soaking was less than for undiluted cells. It was also confirmed with FTPS that the band gap for diluted amorphous silicon is bigger than for undiluted amorphous silicon.

## REFERENCES

- [1] M.J. Powell S.C. Deane, "Defect-pool model and the hydrogen density of states in hydrogenated amorphous silicon" *Physical Review B*, vol. 53 no. 15 1996 pages 10121-10132
- [2] M.J. Powell, S.C. Deane, "Improved defect-pool model for charged defects in amorphous silicon" *Physical Review B*, vol.48 no. 15 1993 pages 10815-10827
- [3] D.L. Staebler, C.R. Wronski, "Reversible conductivity changes in discharge-produced amorphous a-Si" *Applied Physics Letters*, 1977. pages 292-294
- [4] T. Shimizu, "Staebler-Wronski Effect in Hydrogenated Amorphous Silicon and Related Alloy Films" *Japanese Journal of Applied Physics*, vol. 43 2004 pages 3257-3268
- [5] G. van Elzaker, V.Nadazdy et al, "Analysis of structure and defects in thin silicon films deposited from hydrogen diluted silane" *Thin Solid Films*, vol. 511-512 2006 pages 252-257
- [6] J.J.G. van den Heuvel, M. Zeman et al, "Study of the Defect Distribution in a-Si:H during Degradation" *Proceedings of the SAFE/IEEE workshop*, 2000 pages 53-59
- [7] W.B. Jackson, N.M. Amer et al, "Photothermal deflection spectroscopy and detection" *Applied Optics*, vol. 20 no. 8 1981. pages 1333-1344
- [8] A. Mettler, N. Wyrsh et al, "Deep defect determination by the constant photocurrent method (CPM) in annealed or light soaked hydrogenated silicon (a-S:H)" *Solar Energy Materials and Solar Cells*, vol. 34 1994 pages 533-539.
- [9] J.J.G. van den Heuvel, C.S. Kartha et al, "Analysis of dual-beam photoconductivity measurements on light-soaked a-Si:H material" *Proceedings of SAFE*, 2001 pages 66-71
- [10] A. Poruba, M. Vanecek et al. "Fourier transform infrared photocurrent spectroscopy in microcrystalline silicon" *Journal of Non-Crystalline Solids*, 299-302 2002. pages 536-540
- [11] P.R. Griffiths, J.A. Maseth, "Fourier Transform Infrared Spectroscopy" *John Wiley & Sons*, 1986
- [12] P.R. Griffiths, "Chemical infrared fourier transform spectroscopy" *John Wiley & Sons*, 1975
- [13] J. Tauc, "Amorphous and liquid semiconductors" *Plenum*, 1974
- [14] F. Urbach, "The long wavelength edge of photographic sensitivity and of the electronic absorption of solids" *Physical Review*, vol. 92 1953 pages 1324
- [15] B. Abeles, C.R. Wronski et al, "Exponential absorption edge in hydrogenated a-Si films" *Solid State Communications*, vol. 36 1980. pages 537-540
- [16] R. E. L. Schropp, M. Zeman, "Amorphous Silicon and Microcrystalline Silicon Solar Cells: Modleing, Materials and Device Technology" *Kluwer Academic Publishers*, 1998.
- [17] G.D. Cody, "Urbach edge of crystalline and amorphous silicon: a personal review" *Journal of Non-Crystalline Solids*, vol. 141 1992 pages 3-15
- [18] G.D. Cody, T. Tiedje et al, "Disorder and the optical absorption edge of hydrogenated amorphous silicon" *Physical Review Letters*, vol. 47 no. 20 1981 pages 1480-1483
- [19] T. Tiedje, B. Abeles et, "Urbach edge and the density of states in hydrogenated amorphous silicon" *Solid State Communications*, vol. 47 no. 6 1983 pages 493-496
- [20] N.W. Wang, X. Xu et al, "Accuracy of defect densities measured by the constant photocurrent method" *AIP Conference Proceedings*, vol. 234 1991 pages 186-192
- [21] N. Wyrsh, F. Finger et al, "How to reach more precise interpretation of subgap absorption spectra in terms of deep defect density in a-Si" *Journal of Non-Crystalline Solids*, vol. 137-138 1991 pages 347-350

- [22] D. Ritter, K. Weiser, "Suppression of interference fringes in absorption measurements on thin films" *Optics Communications*, vol. 57 no. 5 1986 pages 336-338
- [23] J. Mullerova et al, "Structural and optical studies of a-Si:H thin films: from amorphous to nanocrystalline silicon" *Acta Physica Slovaca*, vol. 55 no. 55 pages 351-359